Research Square

Preprints are preliminary reports that have not undergone peer review.
They should not be considered conclusive, used to inform clinical practice,
or referenced by the media as validated information.

Untargeted LC–MS/MS reveals farming practice- and cultivar-dependent remodeling of the oat grain foodome

Paraskevi Tsermoula
University of Copenhagen
Sarvar A. Kakhkhorov
University of Copenhagen
Søren Balling Engelsen
University of Copenhagen
Kristian Holst Laursen
University of Copenhagen
Bekzod Khakimov
bzo@food.ku.dk

University of Copenhagen

Article

Keywords:

Posted Date: November 9th, 2026

DOI: https://doi.org/10.21203/rs.3.rs-11229959/v1

License: This work is licensed under a Creative Commons Attribution 4.0 International License.
Read Full License

Additional Declarations: No competing interests reported.

Untargeted LC–MS/MS reveals farming practice- and cultivar-dependent remodeling of the oat grain foodome

Paraskevi Tsermoula[a,††], Sarvar A. Kakhkhorov[a,†], Søren Balling Engelsen[a], Kristian Holst Laursen[b], Bekzod Khakimov[a]*

[a]Department of Food Science, University of Copenhagen, Rolighedsvej 26, 1958 Frederiksberg C, Denmark

[b]Department of Plant and Environmental Sciences, University of Copenhagen, Thorvaldsensvej 40, 1871 Frederiksberg C

*Corresponding author: Bekzod Khakimov (bzo@food.ku.dk)

[†] Contributed equally

Abstract

This study investigates the grain foodome of ten oat cultivars grown at two conventional and one organic farming site in Denmark using untargeted LC-MS/MS. More than 1,000 metabolite features were detected, of which >200 were annotated using spectral libraries and computational mass spectrometry tools. Among these, nearly 140 metabolites differed significantly between farming practices, including phenolics, phenolic amides, and steroidal saponins involved in plant defense and stress adaptation. Oat grown under organic practice showed higher levels of hydroxycinnamic acids, avenanthramides, and steroidal saponins, including compounds associated with antioxidant, defense, and anti-inflammatory activities. In addition, 45 metabolites showed cultivar-dependent variation, particularly apigenin-derived flavones, lignans, and lipid-derived metabolites involved in plant signaling and stress responses. Overall, the results reveal distinct metabolic signatures associated with farming practice and cultiva in the oat grain foodome.

Introduction

The continuously increasing global population, together with the loss of arable land driven by climate change, creates an urgent need to produce more food with fewer resources. Plant-based foods provide protein and calories more resource-efficiently than animal products[1] and diets rich in whole grains, vegetables and legumes are associated with health benefits, including reduced risks of heart disease, diabetes and obesity.[2] Therefore, a transition toward balanced diets, rich in plants is one of the most sustainable approaches to support global food security while also improving public health.

Oats (*Avena sativa* L.) are widely consumed cereal grains valued for their nutritional quality and health-promoting properties. Compared to other cereals, oats contain higher levels of protein (11-17%) and lipids (3-7%), but lower levels of carbohydrates (50%), although these values vary with cultivar, environment, and processing.[3] They are rich in the soluble fiber β-glucan,[4] minerals such as potassium, iron, manganese, magnesium and calcium, vitamins including K, E, B1, B2 and B6, as well as sterols and polyphenols,[5] including the avenanthramides, a distinct group of oat phenolics.[6, 7] Oat β-glucan has approved health claims for reducing blood cholesterol, with an intake of at least 3 grams per day being considered sufficient to support this effect and thereby contribute to reduced cardiovascular disease risk.[8, 9] In addition, diets rich in oats have been associated with reduced blood pressure, blood sugar and insulin levels, increased satiety and modulation of the gut microbiota.[10]

With increasing global food demand, current agricultural systems face major sustainability challenges, including resource depletion, biodiversity loss, and environmental degradation. Organic farming seeks to address these challenges through ecological management, circular bioeconomy, and reduced chemical inputs, whereas conventional systems are optimized toward high productivity and are often more reliant to external inputs.[11-13] Oats are well suited to low-input and organic production systems because they require lower fertilizer and pesticide inputs and show higher disease resistance compared to other cereals.[14, 15] Under organic farming conditions, however, plants may experience stronger biotic and abiotic pressures, which can alter gene expression, metabolic pathway activity,

and ultimately grain composition. Metabolomics provides a powerful approach to capture these downstream metabolic responses.[16] Such metabolic shifts can affect the oat grain foodome, both on the levels of nutrients (e.g. amino acids, fatty acids, vitamins) as well as potential antinutrients (e.g. plant secondary metabolites or other unforeseen substances), thereby influencing their nutritional quality.

Characterizing the foodome of oat grains is essential for understanding how genetic and environmental factors shape grain quality. Allwood et al. (2021) reported that nitrogen fertilization across three locations in the United Kingdom increased protein, β-glucan, amino acids, and nitrogen-containing lipids in oat, while reduced avenanthramides levels. They also showed that genotype was a major determinant of oat foodome, with significant varietal differences in amino acids, organic acids, phenolic compounds, saponins, and nitrogen-containing lipids.[17] Similarly, previous studies have demonstrated that genotype influences phenolic content, antioxidant potential, and lipid levels in oats, with hulled oats containing higher levels of phenolic compounds and naked cultivars showing higher lipid content but lower antioxidant activity.[7] Other studies have reported cultivar-dependent differences in fatty acid profiles,[18] as well as in amino acid, phospholipid, coumarin, and terpenoid metabolism.[19] In addition to genotype, farming practice can also modulate oat grain composition. Comparisons of organic and conventional farming systems have shown that organic oats may contain higher avenanthramides concentrations and antioxidant activity, likely reflecting stress-induced stimulation of defense-related pathways, although these responses can depend on genotype.[20-22]

In the present study, we applied an untargeted LC-MS/MS foodomics approach to investigate the variation of low-molecular weight metabolites in ten oat cultivars grown under organic and conventional farming practices at three sites in Denmark. The aim was to identify metabolites and metabolic pathways associated with farming practice- and cultivar-dependent variation and to determine the impact of these factors on the oat grain foodome. Our findings on genotype, farming practice and their interaction-specific changes in grain foodome provide new insight into how plants responds and support future research towards improving oat resilience, and grain quality.

Results

The oat grain foodome

Untargeted LC-MS/MS analysis of the 90 oat grain samples generated a dataset with 1,187 metabolite features. Of these, 121 features were annotated at level 2[23] by matching accurate mass, MS/MS fragmentation patterns, and isotopic patterns against spectral libraries implemented in MetaboScape 2021b. In addition, 194 features were tentatively annotated at level 3[23] using SIRIUS. Overall, 299 annotations were obtained at levels 2 and 3, including 33 features uniquely annotated by MetaboScape, 90 uniquely annotated by SIRIUS, and 88 consistently annotated by both approaches. After removing redundant annotations, the final annotated dataset comprised 228 unique metabolites, which were assigned to eight chemical classes: lipids (n = 81), heterocyclic compounds and alkaloids (n = 38), phenolic compounds and derivatives (n = 33), amino acids and peptides (n = 23), terpenoids (n = 20), carbohydrates (n = 10), polyketides (n = 7), and miscellaneous compounds (n = 16). The remaining 888 features were retained as unannotated features.

All 1,187 LC-MS/MS features were subjected to ANOVA-simultaneous component analysis (ASCA) to evaluate the effects of farming practice and cultivar on the oat grain foodome (Fig. S1). The farming practice factor included three levels: Gamborg and Sejet, representing conventional farming practices, and Hammel, representing organic farming practices. Cultivar comprised ten levels: Caddy, Delfin, Dominik, Galant, Lion, Max, NORD 20/127, NORD 20/223, Oskar, and Scotty. Both farming practice and cultivar had significant effects on the oat grain foodome, explaining comparable proportions of variation, 13.8% and 13.7%, respectively ($p = 0.001$). When the analysis was restricted to the 228 level 2 and 3 annotated metabolites, the explained variation associated with farming practice increased to 28.1% ($p = 0.001$), whereas the cultivar effect remained at a similar level, explaining 17.5% of the variation ($p = 0.001$) (Fig. 1).

Effect of farming practice on oat grain foodome

The ASCA scores plot based on all 1,187 LC-MS/MS features showed a clear separation of oat samples according to farming practice (Fig. S1a). Along simultaneous component 1 (SC1), which explained 86% of the variation associated with farming practice, samples from Hammel, representing the organic farming practice, were clearly separated from those from Gamborg and Sejet, representing the conventional farming practice. The partial separation of the two conventional sites was observed along SC2, which explained the remaining 14% of the variation related to the farming practice and partly distinguished the two conventional sites from each other. These results indicate that the main difference in foodome was between oats grown under organic farming practice and those grown under conventional farming practice.

The corresponding ASCA loadings plot (Fig. S1b) indicate that numerous metabolites contributed to the observed separation. However, because of the high number of overlapping variables, visual interpretation of the loadings was challenging. To obtain a clearer overview of the metabolites driving the separation due to the farming practice, ASCA was repeated using only the 228 metabolites annotated at levels 2 and 3 by MetaboScape and SIRIUS. The ASCA scores plot for the farming practice effect showed that it accounted for 28.1% variation ($p = 0.001$), with SC1 separating the samples grown under organic farming at Hammel from those grown under conventional farming at Gamborg and Sejet (Fig. 1a).

Mapping the normalized ASCA loadings onto the molecular network allowed to connect the statistical contribution of individual features with their structural relationships. Therefore, the normalized SC1 loadings were projected onto the molecular network of annotated metabolites to identify the chemical fingerprints separating the oats grown under organic farming from those grown under conventional farming (Fig 1c). Nodes with strongly positive loading values (red nodes in network) corresponding to samples grown under organic farming included hydroxycinnamic acid amides, particularly the oat-specific avenanthramides, including anenanthramides 2p, 2f, 2c, 2fd, 2pd, 3f, and

5f, and the hydroxycinnamoyl serotonin conjugates N-feruloylserotonin and N-caffeoylserotonin. Other metabolites belonging to the phenylpropanoid pathway such as coumarin, chromone, methoxychromone, ferulic and coumaric acids were also specific to Hammel samples. Aglycones of nuatigenin-type steroidal saponins common in oats contributed to the separation of samples from organic farming, while their glycosylated analogues were more specific to conventional farming. Several N-heterocyclic compounds and alkaloids, including xanthine, uridine and uracil and the purine metabolites uric acid adenosine, and guanosine were also associated with organic farming samples. Similarly, amino acids, the peptide glutathione, phosphoethanolamines (PEs), and phosphocholines (PCs) with one fatty acid chain (i.e. linoleoyl glycerophosphoethanolamine (PE 18:2), tetradecanoyl glycerophosphoethanolamine (PE 14:0), octadecatrienoyl glycerophosphoethanolamine (PE 18:3), and lauroyl glycerophosphocholine (PC 12:0), glycerophosphocholine, palmitoyl glycerophosphocholine (PC 16:0), palmitoleoyl acetyl glycerophosphocholine (PC 16:1/2:0), respectively) were more specific to organic farming. In contrast, PEs with two fatty acid chains, such as dilinoleoyl phosphatidylethanolamine (PE 18:2/18:2) and linolenoyl-linoleoyl phosphatidylethanolamine (PE 18:3/18:2), and PCs with shorter fatty acid chains were more related to conventional farming.

In addition, normalized SC2 loadings were mapped onto the molecular network to identify the chemical fingerprints distinguishing oats grown at Gamborg from those grown at Sejet under conventional farming (Fig S2). Nodes with strongly positive loading values (red nodes in the network), corresponding to the Gamborg samples, including the purine metabolites deoxyadenosine, adenosine, methylthioadenosine, and uridine; the carbohydrates maltotetraose, maltotriose, and branchiose; PCs containing one and two fatty acyl chains, including PC 18:1/18:2, PC 14:0/20:1, and PC 18:2/18:2; fatty acid derivatives such as 9-oxo-C18:3 and C18:3 amide; and other metabolites such as tryptophan, N-acetylserotonin, methylquinoline and vanillin. In contrast, nodes with strongly negative loading values (blue nodes in the network), corresponding to the Sejet samples, included flavonoids (tricin, vitexin,

and vicenin 2), flavanolignans (salcolin A, salcolin A acetate, and calquiquelignan D), homopipecolic acid and steroidal saponins.

Impact of farming practice on individual metabolites and metabolites classes

Effect of the farming practice on individual metabolites was further assessed using one-way ANOVA. In total, 142 out of 228 annotated metabolites were significantly different between the organic and conventional farming practices (FDR-adjusted $p < 0.05$). A heatmap of the top 50 most significant metabolites revealed two major metabolite clusters (Fig. 2a). The first cluster contained metabolites with higher levels in the samples from the conventional farming. Within this cluster, oxopentadecadienal, 9-glycero-9-oxo-C9:0, and 8,17-dihydroxylinoleic acid (diOH-C18:2) formed one subcluster, whereas vanillin grouped with nuatigenin-3-O-Glc, nuatigenin-3-O-Glc, 26-O-Glc and cyclitol.

The second major cluster contained 40 metabolites that were consistently more abundant in organic farming samples, with the exception of homopipecolic acid, 26-desglucoavenacoside C, 3-oxonuatigenin and N-feruloylserotonin, which were more abundant in the organic farming samples and in the samples from the conventional farming in Sejet. This cluster included three subgroups. One subgroup included homopipecolic acid and 26-desglucoavenacoside C, which were associated with phenolic and indolic compounds, such as 7-methoxychromone, coumaric acid, 2-methylquinolin-8-ol, 8-methoxykynurenate, 3-oxonuatigenin and N-feruloylserotonin. These metabolites were further associated with amino acids (i.e. carnitine, leucine, methionine), dodecanoyl-glycero-phosphocholine (LysoPC 12:0), methylthioadenosine, 4-hydroxycinnamide and erythrosphiganine. The second subgroup included ferulic acid, avenanthramides 3f, 2p, 2f, and 5f, nuatigenin and avenocoside C together with three additional phenolic compounds. The third subgroup included hydroxycoumarin, avenanthramides 2c, and 2pd, hydroxy-naphthoic acid, and oxo-octadecadienoic acid, which clustered together with N-caffeoylserotonin, niacin, avanathramide 2fd, an open-chain polyketide, acyl platelet-activating factor and urate.

Oat-specific secondary metabolites affected by farming practice

Among the metabolites significantly increased in the organic farming samples, the oat-specific avenanthramides and nuatigenin- and furostane-type steroidal saponins were of particular interest (Fig. 2b). Seven avenanthramides were detected, namely avenanthramides 2p, 2f, 2c, 3f, 2fd, 2pd, and 5f (Fig. 4, Fig. S4b). These compounds were strongly affected by farming practice, with effect sizes ranging from 64.5% to 89.7%. Avenanthramide 2c showed the strongest effect, with an effect size of 89.5% ($p = 7.73 \times 10^{-42}$). Overall, avenanthramides were most abundant in Hammel samples, present at very low levels in Gamborg samples, and slightly higher in Sejet samples.

Three additional features from hydroxycinnamic acid amide molecular network could not be assigned as established oat avenanthramides (Fig. 4). The feature at *m/z* 314.1020 produced a dominant fragment ion at *m/z* 147.0439 consistent with coumaric acid moiety typically resulted from amide bond cleavage connecting hydroxycinnamic acid moieties to anthranilic acid moieties in avenanthramides (Fig. S3a). Neutral loss of 167.058 Da corresponds to methoxyanthranilic acid and it was therefore assigned only at the substructure level as a putative *N*-coumaroylmethoxyanthranilic acid isomer. The feature at *m/z* 272.0916 was tentatively annotated as *N*-benzoyl-4-methoxyanthranilic acid also known as methoxydianthramide B, a dianthramide phytoalexin produced by carnation plants (*Dianthus caryophyllus* L.).[24] It has been established that in carnation, the biosynthesis of *N*-benzoyl-4-methoxyanthranilic acid is initiated by hydroxycinnamoyl/benzoyl-CoA *N*-hydroxycinnamoyl/benzoyltransferase (HCBT; EC 2.3.1.144), which condenses benozyl-CoA with anthranilate to form *N*-benzoylanthranilate before subsequent hydroxylation and O-methylation. The enzyme was also shown to accept salicyloyl-CoA in vitro. Accordingly, the feature at *m/z* 288.0860 was tentatively assigned as an *N*-salicyloylmethoxyanthranilic acid isomer. However, neither benzoylated nor salicyloylated methoxyanthranilic acid conjugates have been previously reported in oats because no HCBT gene or corresponding benzoyl-CoA *N*-benzoyltransferase activity has, to our knowledge, been characterized in oats (*Avena sativa* L.). Oat avenanthramides are instead assembled by hydroxycinnamoyl-CoA:5-hydroxyanthranilate *N*-hydroxycinnamoyltransferase (HHT; EC 2.3.1.302),

which forms the amide bond between the two avenanthramide moieties by transferring *p*-coumaroyl-CoA or caffeoyl-CoA to 5-hydroxyanthranilic acid yielding avenanthramides 2p and 2c, respectively.[25] Avenanthramide 2f is subsequently produced through the methylation of avenanthramide 2c mediated by caffeoyl-CoA *O*-methyltransferase rather than by direct HHT-catalyzed conjugation of feruloyl-CoA. Therefore, the annotation of benzoylated and salicyloylated methoxyanthranilic acid conjugates in oat remain not supported biochemically unless they are confirmed using authentic standards.

A similar pattern was observed for several nuatigenin-type steroidal saponins and sapogenins. 3-oxonuatigenin showed a strong farming practice effect, with an effect size of 82.5% ($p = 2.50 \times 10^{-32}$), while nuatigenin showed an effect size of 59.9% ($p = 3.81 \times 10^{-17}$). 3-Oxonuatigenin was particularly abundant in organic farming samples, with a ~1.10-fold lower abundance in conventional faming samples. In contrast, nuatigenin-3-O-Glc exhibited the opposite trend, with higher levels in conventional faming samples than in organic farming samples (effect size = 58.0%, $p = 2.27 \times 10^{-16}$). Finally, N-caffeoylserotonin, a hydroxycinnamoyl serotonin conjugate, was enriched in organic farming samples (effect size = 75.4%, $p = 3.82 \times 10^{-2}6$) and was absent from the majority of conventional faming samples.

Effect of cultivar on oat grain foodome

ASCA showed that cultivars explained a significant proportion of the variation in the oat grain foodome, both using the full LC-MS/MS feature dataset (Fig. S1c) and the annotated metabolite dataset (Fig. 1c), explaining a substantial proportion of the variation (13.7%, p = 0.001 and 17.5%, p = 0.001, respectively). Despite the effect size, the scores plot based on all 1,187 LC-MS/MS features showed considerable overlap among cultivars. In contrast, the annotated metabolite dataset resulted in partial separation of the cultivars. Although Lion and Max cultivars overlap, these together with Dominik are separated from the remaining cultivars along SC1, which explain 22% of the variation.

Normalized ASCA loadings along SC1 were mapped onto the molecular network of annotated metabolites (Fig. 1d). The ASCA scores plot for cultivar effect showed that Dominik cultivar is related with positive loading values, while Lion and Max with negative loadings values. In contrast to the phenylpropanoid pathway metabolites affected by the farming practice, the flavonoids and flavanolignans are influenced by the cultivar effect. In particular, metabolites with extreme negative SC1 loadings including isovitexin 2-O-arabinoside, vitexin, tricin, salcolin A, salcolin-A-acetate, and calquiquelignan D, are more abundant in the Lion and Max cultivars. In contrast, vicenin 2 had strongly positive loadings value showing that it is a characteristic of Dominik cultivar. Among the metabolites with high positive loading values were fatty acids and their oxidation products, fully glycosylated steroidal saponins including sativacosides A and C and avenacoside A. Taking into account that the cultivar × farming practice interaction was significant ($p = 0.002$) and explain 15.1% variation, these results indicate that although cultivar had a measurable influence on oat grain composition, its effect is modulated by farming practice. In particular, farming practices affect the up- or downregulation of metabolic signatures specific to cultivar.

Variations of individual grain metabolites across oat cultivars

One-way ANOVA with FDR correction identified 45 of the 228 annotated metabolites as significantly different among oat cultivars, independently of the farming practice effect (FDR-adjusted $p < 0.05$). The relative abundances of these 45 cultivar-associated metabolites are shown in a heatmap with hierarchical clustering (Fig. 3a), which revealed two major metabolite clusters corresponding to 3 metabolite classes.

Flavonoids, flavanolignans and lignans

In the first cluster, a cultivar-specific pattern was observed for several flavonoid- and phenylpropanoid-related metabolites. Isovitexin-2-O-arabinose and tricin are present at low levels in most cultivars, but are increased in Lion and Max. Salcoline A, calquiquelignan D, salcolin A acetate, calquiquelignan D, and vitexin are detected at low abundances in Oskar, Scotty, Caddy, and Galant,

showed intermediate abundances in Dominik, Delfin, and NORD 20/127, and reach their highest levels in Lion and Max. These metabolites are closely associated with vicenin 2, isoquinoline, N-benzoyl-4-methoxyanthranilate and dianthalexin. Vicenin 2 and isoquinoline were most abundant in Oskar and showed intermediate levels in NORD 20/223, whereas N-benzoyl-4-methoxyanthranilate and dianthalexin were most abundant in Dominik and occurred at very low levels in the remaining cultivars.

Lipid-derived metabolites and associated stress compounds

The second major cluster contained 35 metabolites organized into two subclusters. The first subcluster contained the osmolytes pipecolic acid and homopipecolic acid and the nucleoside adenosine together with the methionine salvage/polyamine metabolism intermediate methylthioadenosine. These metabolites are also related to deoxydesglucoavenocoside A and methylquinoline. This subcluster was associated with lipid oxidation and hydrolysis products, including oxidized fatty acids, such as 9-oxo-linoleic acid (9-oxo-C18:2), 4-hydroperoxy-2-nonenal, and 8-(3-octyl-2-oxiranyl)-octanoic acid. These lipid derivatives showed highest levels in Dominik and NORD 20/127, intermediate levels in NORD 20/223, while the remaining cultivars exhibited the lowest levels. The second subcluster included the amino acids histidine, aspartic acid, and sarcosine, together with several lipid-related metabolites, including the lysophosphatidylethanolamine (LysoPE) 14:0, 9,10-dihydrojasmonic acid, linoleoyl ethanolamide and the sphingolipids sphingosine and phytosphingosine. This subcluster is associated with the sesquiterpene vomifoliol, monoacylglycerols including monoolein and monolinolein, and nuatigenin-based steroidal sapogenins all of which showed highest levels in Dominik.

Cultivar dependent variation in flavonoids and lignans accumulation in oat grain

The cultivar-dependent trends of selected flavonoids and flavonoid conjugates observed in the heatmap are further illustrated by boxplots in Fig. 3b. Vicenin 2 show the strongest cultivar effect, with an effect size of 95% ($p = 3.31 \times 10^{-48}$). This compound is most abundant in Dominik and Galant

and is detected in very low abundancies in rest of cultivars. Tricin is the most abundant flavonoid among the selected compounds and also show a strong cultivar effect, with an effect size of 90.5% ($p = 4.17 \times 10^{-37}$). Tricin levels were highest in Max, but is absent in Caddy, Galant, Oskar, and Scotty. Vitexin, a flavone glucoside, also displayed strong cultivar dependency, with an effect size of 81.5% ($p = 9.30 \times 10^{-26}$), it was not detected in Caddy, Scotty, and Dominik and showed the highest concentration in Max. Oskar showed low vitexin concentration, whereas the remaining cultivars had no detectable levels. A similar trend was observed for the flavone glycoside isovitexin-2-O-arabinose, which showed an effect size of 72.0% ($p = 1.07 \times 10^{-18}$). This metabolite was most abundant in Lion and Oskar, while the remaining cultivars showed similarly low levels. It is also noteworthy that the phenylpropanoid-derived lignans salcolin A, salcolin A acetate, and calquiquelignan D showed similar accumulation patterns across cultivars. These metabolites are most abundant in Lion, Max, NORD 20/127, and NORD 20/223, suggesting that specific oat genotypes may be characterized by enhanced accumulation of flavonoid and lignan-related metabolites.

Discussion

Conventional farming practices rely on synthetic fertilizers and pesticides, prioritize high yield and have been associated with production of grains of lower nutritional density.[26] In contrast, organic farming depend on organic (circular) fertilizers and crop management but faces challenges such as variable nutrient availability, weed pressure and biotic stress.[13] These conditions can trigger plant signaling and metabolic adaptations, which in oats have been linked to the production of grains with higher nutrient density.[27] In this context, oats are gaining increasing attention as a potential sustainable crop and a key component of plant-based nutrition due to its high content of bioactive compounds and nutritional profile.

Oats are more resilient than temperate cereals, low-input crops that can maintain productivity under variable nutrient availability and show cultivar-dependent tolerance to abiotic stress and resistance to biotic stress.[14, 28] Under organic management, this resilience has also been associated with higher

concentrations of secondary metabolites, including phenolic compounds and avenanthramides, with documented nutritional and health benefits.[29] Our results show that oats grown organically in Hammel site contained higher levels of phenolics, oat specific phenolic amides, steroidal sapogenins, saponins and indole derived metabolites than the conventionally grown oats from Gamborg and Sejet.

At metabolic level, adaptation to possible stress from organic farming practice is associated with changes in the expression of biosynthetic pathways. One such pathway in this study is the phenylpropanoid pathway, which is a primary source of secondary metabolites mediating defense responses in plants. The increased levels of 4-hydroxycinnamide, N-feruloylserotonin, N-caffeoylserotonin, ferulic and coumaric acid in Hammel samples (Fig. 2b) indicate stimulation of this pathway in response to the organic farming conditions.[30] Hydroxycinnamic acids and their amides have been reported to strengthen cell walls and to act as antimicrobial agents protecting plant cells against pathogen invasion.[31, 32] In wheat, for example, N-caffeoylserotonin and N-feruloylserotonin have been proven to increase cell wall thickness to resist *Fusarium graminearum*.[33]

In addition to hydroxycinnamic acids and their derivatives, oats rely on saponins for their defense.[34] Saponins are mainly characterized by their antimicrobial, anti-cytotoxic, anti-inflammatory, anti-cancer properties and to lesser extend their insecticidal properties.[35-37] In particular, nuatigenin-type steroidal saponins are unique to oats with furostane-type steroidal saponins having been recently described in oat grains (Figure 5).[27, 38] Their structural diversity is primarily driven by differences in number, composition, and linkage of glucose and rhamnose moieties attached at C3 and C26, along with variation in C25 stereochemistry. Notably, the steroidal saponins were not annotated by the available spectral libraries. Their detection instead relied on the complementary use of SIRIUS structural prediction and GNPS suspect library[39] matching, which enabled prioritization of candidate saponin structures. The resulting annotations were subsequently evaluated manually by comparison of their overall MS/MS fragmentation pattern with the experimentally confirmed spectra previously reported in the literature. In positive ion LC-MS, nuatigenin-type saponins are generally detected as intact protonated or ammoniated molecular ions, while furostane-type saponins undergo dehydration

involving the C22 -OH group and may therefore be observed as $[M+H-H_2O]^+$ ion.[40, 41] Accordingly, sativacosides B, A, and C were detected at *m/z* 1209.59, 1047.5376, 885.4841, respectively, corresponding to their dehydrated protonated ions (Fig. 5b). Nuatigenin-type avenacosides characteristically yield protonated nuatigenin at *m/z* 431.3154, while furostane-type sativacosides may yield protonated aglycone at *m/z* 433.2572 reflecting 2.0156 Da difference between the two aglycones (or at *m/z* 415.3182 corresponding to dehydrated aglycone due to -OH group loss at C22). Sativacoside B and avenacoside B were not included in Fig. 5 because they were detected predominantly as $[M+2H]^{2+}$ and no valid MS/MS spectra were acquired for these features. The observed differences in nuatigenin-type steroidal saponins between the farming practices suggest that biotic stress plays a key role in shaping their profiles. The increased levels of nuatigenin mono and diglucosides in samples from conventional farming may indicate reduced microbial activity due to pesticide application. This could limit the hydrolysis of sugar moieties, resulting in slower or incomplete microbial detoxification. In contrast, organically grown oats are susceptible to pathogens, which can lead to hydrolysis of sugar moieties and shift the profile of nuatigenin-type steroidal saponins toward aglycones in Hammel samples. This observation aligns with previous findings that fungal enzymes such as α-rhamnosidase and β-glucosidase can detoxify saponins through sequential sugar hydrolysis.[42]

Another group of secondary metabolites specific to oats that were influenced by farming practice were avenanthramides. They are major free phenolic compounds in oats synthesized in response to pathogen attack or environmental stress.[43] It has been suggested that they are *de novo* synthesized through a hydroxycinnamoyl-CoA: hydroxyanthranilate N-hydroxycinnamoyl transferase.[44] The profile of avenanthramides varies with genotype and growing environment, with fungal pathogens, diseases and chemical elicitors being known to stimulate their biosynthesis.[45] Accumulation of avenanthramides in oat groats has been shown to be mainly influenced by growth conditions rather than different genotypes and their accumulation in oat grains is higher when the farming location is crown rust infected.[46] These observations are in accordance with our results, where the annotated

avenanthramides had low levels in samples from conventional farming, while they accumulated to higher levels in samples from organic farming (Fig. 2). In particular, avenanthramide 2p was 2.4- and 1.5-fold higher, avenanthramide 2c 3.1- and 2.0-fold higher, avenanthramide 2f 1.9- and 1.3-fold higher, avenanthramide 3f 1.8- and 1.1-fold higher, avenanthramide 2pd 3.1- and 1.8-fold higher and avenanthramide 2fd 2.3-fold higher in the organic samples. However, since organic cultivation usually subjects plants to biotic and abiotic stress, the increased avenanthramide accumulation observed in organic cultivation could be associated with differences in farming practices. Since organic cultivation was represented by only one location in a single year, the effects of farming practices cannot be separated from the location effects. Although the findings suggest that organic practices may favor avenanthramide accumulation in Hammel samples, it requires confirmation across multiple locations and years.

The main metabolites responsible for differentiating oat cultivars were involved in lipid and phenylpropanoid metabolism, including metabolites of plant stress response. In plants, lipids and their derivatives serve as structural components of cellular membranes and energy reserves[47] but also as precursors of signaling molecules involved in development and responses to biotic and abiotic stress.[48] In addition, metabolites of the phenylpropanoid pathway have antioxidant activity and are involved in signaling and adaptation to environmental stressors.[49] Therefore, the observed metabolic variation points toward regulation of these pathways at cultivar level, independent of farming practice, that contributes to differences in biochemical composition and stress responses among oat cultivars.

Oats have a high lipid content (typically 3-7%) compared to other cereals, and with a relative high proportion of unsaturated fatty acids.[50] The main unsaturated fatty acids (UFAs) in oats are palmitic (C18:0), oleic (C18:1) and linoleic (C18:2) acids, represent 90-95% of all fatty acids,[50] which are substrates for oxidative and enzymatic pathways that generate signaling molecules, including 13-keto-C18:2, 9-oxo-C18:2, 9-oxo-C18:3(2) and diOH-C18:2, 9,10-dihydrojasmonic acid, azelaic acid, linoleoyl ethanolamide, sphingosine, phytosphingosine and 4-hydroperoxy-2-nonenal, involved in stress adaptation and immune responses. Oxidative hydrolysis of unsaturated fatty acids generates a range

of oxidation products, including azelaic acid, which acts as a priming molecule in systemic acquired resistance (SAR).[51] In addition, enzymatic oxidation of polyunsaturated fatty acids by lipoxygenases generates oxylipins, including 13-keto-C18:2, 9-oxo-C18:2, 9-oxo-C18:3(2) and diOH-C18:2, that mediate stress response and innate immunity.[52] As shown in Fig. 3a and b, Dominik exhibited the highest levels of these lipid derivatives, whereas Max and Delfin showed 0.8 and 0.6-fold lower levels, with the remaining cultivars displaying intermediate profiles. Their variation among the cultivars reflect not only differences in fatty acid composition, but also differences in the activity of oxidative pathways.[53]

However, accumulation of ROS can also lead to cellular damage and necrosis and therefore, plants regulate ROS levels to sustain immune responses without compromising tissue integrity. Sphingolipids contribute to this regulation and thus variation of phytosphingosine levels (Fig. 3a) shows the potential of oat cultivars to activate sphingosine kinase for the biosynthesis of phosphorylated sphingolipids, which support ROS detoxification and restrict pathogen progression and promote SAR development.[54, 55] In addition to regulation of ROS by sphingolipids, differential accumulation of LysoPE and monoacylglycerols among the oat cultivars (Fig. 3a) indicates membrane remodeling associated with stress adaptation. Lysophospholipids such as LysoPE induce expression of genes involved in plant defense,[56] while monoacylglycerols, including monoolein, monolinolein and monolineoyl, are products of triacylglycerol catabolism, indicate lipid turnover that provides both metabolic energy and signaling intermediates.[57]

Distinct accumulation patterns of flavonoids and lignan metabolites among oat cultivars indicate differences in the regulation and metabolic flux of the phenylpropanoid pathway.[58] Several glycosylated derivatives of apigenin, quercetin, kaempferol and tricin were annotated, including apigenin C-glycosides vitexin and vicenin 2, and the C-glycoside-O-glycoside isovitexin-2-O-arabinoside compounds belonging to flavone glycosides previously described in *Avena sativa*.[59] In this study, we show that only Dominik and to less extent Galant oat samples contained vicenin 2 suggesting that the cultivars have distinct di-C-glycosylation capacity.[60] In contrast, the mono-C-

glycoside vitexin was highest in Max, lower in Lion and the NORD lines, and further reduced in Galant and Oskar. Similarly, isovitexin-2-O-arabinoside accumulated in Lion and Max, while the remaining cultivars showed lower levels. This contrasting distribution suggests potential cultivar-dependent partitioning of apigenin metabolism between the di-C-glycosylated branch and mono-C-glycosylated products that can undergo further O-glycosylation. In cereals, flavone C-glycosides are synthesized through CYP93G-family flavanone 2-hydroxylases (F2H) followed up by UDP-sugar-dependent C-glycosylation of 2-hydroxyflavanone intermediates and subsequent dehydration, while formation of isovitexin-2-O-arabinoside additionally requires O-arabinosylation of the C-bound glucose.[59, 61] the relative accumulation of mono- and di-C-glycosylated products is influenced by the expression, substrate specificity, and regioselectivity of the C-glycosyltransferases along with precursor availability and downstream pathway flux. C-glycosylation generates flavones resistant to hydrolysis, while additional glycosylation of C-bound sugars can further modulate their solubility, transport, sequestration, and turnover. Therefore, the prevalent accumulation of vicenin 2 may represent stronger metabolic predisposition towards a stable di-C-glycosylated apigenin pool in cultivars. Such cultivar-specific glycosylation patterns may influence how flavones are stored and spatially deployed for functions including antioxidant defense, UV protection, and abiotic stress tolerance.[58]

Tricin and the putatively annotated lignan metabolites salcoline A, salcoline A acetate and calquiquelignan D show further diversification of phenylpropanoid metabolism among cultivars. To our knowledge these compounds, except tricin, have not been previously reported in oats, although tricin-derived flavonolignans such as salcolins have been described in plants and tricin derivatives occur as lignans and lignan glycosides in plant tissues.[62] Tricin has been reported in oats[58] and is linked to lignification as it can be incorporated into lignin polymers and contribute to cell wall strengthening.[63] Oat tissues also contain tricin-derived flavonolignans, supporting a structural branch from flavone to flavonolignan metabolism.[64] In our dataset, the highest levels of tricin and these putative lignan-related annotations were observed in Lion and Max, while their abundance was very

low in Caddy and Oskar. This distribution suggests cultivar differences in the allocation of phenylpropanoid carbon toward structural metabolites.

The present study demonstrates that both farming practice and cultivar type, influence the detailed oat foodome. Across the ten cultivars analyzed, the main differences were associated with lipid, phenylpropanoid, and steroidal saponin pathways, indicating that composition of oat grains reflects metabolic changes related to plant defense and stress adaptation, with potential implications for their nutritional quality. Among the cultivars, Dominik showed the most distinct metabolic profile and showing significant differences in lipid metabolites associated with stress response and phenylpropanoid metabolism.

These results demonstrate that, while genetic improvement through breeding remains central to crop improvement, farming practices and growing environment can also substantially modulate the oat grain foodome. Pronounced variation in avenanthramides, steroidal saponins and other defence- and stress-related metabolites across farming practices, together with cultivar-dependent differences in flavonoid, phenylpropanoid and lipid metabolism, highlights the combined influence of genetic background and growing conditions on grain composition. Thus, crop improvement could benefit from considering both genetic traits and their metabolic responses to agricultural management and environment, particularly in relation to plant resilience and grain quality. However, this study covered a single growing year, with organic farming represented at only one location, preventing farming practice effects from being fully separated from location-specific effects. Future multi-year and multi-location studies integrating agronomic and environmental data are therefore needed to disentangle genotype, management and environment effects and identify robust metabolic traits for developing resilient oat cultivars with improved grain quality.

Methods

Field trials and samples

Ten cultivars of oats (*Avena sativa* L.), Caddy, Delfin, Dominik, Galant, Lion, Max, NORD 20/127, NORD 20/223, Oskar, and Scotty, were grown at 3 different geographic locations in 2022 (30 samples in total). At two locations (Sejet and Gamborg), oats were grown according to conventional principles. Sejet is a clay loam/heavy clay soil while Gamborg is a silty loam/clay loam soil. Oats were sown March 25th or March 21st at Sejet and Gamborg, respectively. At Sejet, oats received 70 kg N per hectare on March 23 and 40 kg N per hectare on May 6, supplied as 21-4-10 synthetic NPK fertilizer, while at Gamborg, oats received 66 kg N per hectare on March 20 and 64 kg N per hectare on April 1, supplied as 18-5-11 synthetic NPK fertilizer. At Sejet and Gamborg pesticides were applied to control weeds, fungi and pests. In addition, the micronutrient manganese was applied 2-3 times during the growth season. At Hammel, where the soil is coarse sandy clay, oats were grown according to the principles of organic farming (EU Regulation 2018/848). Sowing was conducted on the 12th of May and no fertilizers or pesticides were applied. At maturity, ultimo August/primo September, oats were harvested and stored in aerated bags.

Sample processing

All oat samples were extracted and analyzed in triplicate. For each oat sample, three independent technical extractions were performed in randomized order using 80% methanol (HPLC-grade, Sigma-Aldrich, Germany) in 2 mL Eppendorf tubes. The extraction solvent was supplemented with 4 µM sulfadimethoxine (VETRANAL™, analytical standard, Sigma-Aldrich, Germany) which served as an internal standard for monitoring LC-MS/MS system performance. Samples were vortex-mixed (Vortex-Genie 2, Scientific Industries, USA) for 10 seconds and subsequently ultrasonicated (Sonorex Digitec DT 100 H, Bandelin, Germany) at 35–40 °C for 30 minutes. The samples were vortexed again for 10 seconds and centrifuged (ScanSpeed 1580R, LaboGene, Denmark) at 21,124 × g for 20 minutes at 4

°C. Subsequently, 200 µL of supernatant was transferred to glass inserts (Mikrolab Aarhus A/S, Denmark) placed in 2 mL glass vials (Mikrolab Aarhus A/S, Denmark).

LC-MS/MS data acquisition

Extracted samples were analyzed in randomized order using an Elute ultra-high-performance liquid chromatography (UHPLC) system coupled to an impact II quadrupole time-of-flight mass spectrometer (QTOF-MS) (Bruker Daltonik, Bremen, Germany). Pooled quality control (QC) and blank samples were included after every eight samples. Chromatographic separation was performed using a reverse-phase Intensity Solo 2 C18 column (100 Å, 2 µm, 100 mm × 2.1 mm, Bruker Daltonik) preceded by an ACQUITY UPLC BEH C18 VanGuard pre-column (130 Å, 1.7 µm, 2.1 mm × 5 mm, Waters Corporation, Milford, MA, USA), maintained at 40 °C. The mobile phase consisted of Milli-Q water + 0.1% formic acid (Merck, Germany) and acetonitrile + 0.1% formic acid (hypergrade LiChrosolv®, Merck, Germany) delivered at a constant flow rate of 0.3 mL/min. The chromatographic gradient was programmed as follows: 0–2 min, 100% A; 2–8 min, linear gradient to 100% B; 8–11 min, 100% B; 11–11.01 min, return to 0% B; and 11.01–14 min, re-equilibration at 0% B.

Mass spectra were acquired over an *m/z* range 20 to 1300 at a spectral rate of 12 Hz using electrospray ionization (ESI) in positive-ion mode. Prior to sample analysis, the instrument was externally calibrated using a 10 mM sodium formate solution in 50% isopropanol before sample analysis and tuned with ESI-L Low Concentration Tuning Mix (Agilent Technologies, Santa Clara, CA, USA). ESI conditions were: end plate offset: 500 V, capillary voltage: 4500 V, nebulizer pressure: 2.2 bar, dry gas flow: 10 L/min, and drying temperature: 220 °C. MS conditions were: funnel 1 and 2 RF: 200 Vpp, hexapole: 50 Vpp, ion energy: 5 eV, collision energy: 5 eV, pre-pulse storage: 5 µs. Tandem mass spectra were acquired in data-dependent acquisition mode with three precursor ions selected per scan cycle. Active exclusion was applied after three spectra and a release period of 0.20 min. LC-MS/MS acquisition was controlled using otofControl v5.2 and Bruker Compass HyStar v5.1 (Bruker Daltonik).

Data analysis

Prior to statistical analysis, the LC-MS/MS data were prerpocessed with MetaboScape 2021b (Bruker Daltonik). Feature extraction parameters comprised a minimum feature occurrence in ≥2 analyses, minimum presence in ≥3 analyses, intensity threshold of 5000 counts, and a minimum peak length of six spectra, reduced to four spectra during recursive extraction. Extracted ion chromatogram (EIC) correlation was set at 0.8, considering ions: $[M+H]^+$, $[M+Na]^+$, $[M+K]^+$, $[M+NH_4]^+$, $[M+H-H_2O]^+$, $[2M+H]^+$, $[M+H+H]^{2+}$, and $[M]^+$, with $[M+H-H_2O]^+$ as a common fragment ion. Mass recalibration was performed using the auto-detection (Na Formate pos) function. Spectral annotation employed hierarchical search mode, with annotations accepted exclusively by MS/MS spectra. Precursor *m/z* tolerances of 2–5 ppm, mSigma tolerances of 20–50, and MS/MS scores ranging from 600 to 900 were applied.

Feature-based molecular networking (FBMN, v2024.10.09) was performed within the GNPS2 ecosystem (gnps2.org), applying a precursor ion tolerance of 0.05 Da, fragment ion tolerance of 0.05 Da, cosine score, and minimum matched peaks set at 0.65 and 6, respectively. Molecular networks were visualized using Cytoscape v3.10.4. Complementary computational annotation was performed using SIRIUS (v6.0.6) employing CSI:FingerID for molecular structure predictions and the top-ranked candidates were assigned COSMIC confidence scores ranging from 0 to 1.

ANOVA-simultaneous component analysis (ASCA) and one-way ANOVA were performed in MATLAB R2021b using scripts written by the authors. Analyses were performed on autoscaled data, and p-values were adjusted for multiple testing using the Benjamini–Hochberg procedure (FDR = 5%). The ASCA model included cultivar, farming practice and their interaction, with significance assessed by permutation testing (n = 1000). ANOVA was performed on individual metabolite features to assess differences among cultivars and farming practice. Hierarchical clustering for heatmaps was performed using Ward's method and Euclidean distance on row-wise max-normalized data.

Data availability

The data supporting this article is available through https://github.com/BEKZODKHAKIMOV/LC-MS-based-Oat-Metabolomics. Untargeted LC-MS/MS data generated for this study are publicly available at Global Natural Products Social Molecular Networking (GNPS)/MassIVE under the accession code MSV000100540. Molecular networking job can be accessed at: https://gnps2.org/status?task=9a91112f7a6a40a5ad2297ffa22c9ad3

Acknowledgements

We thank the AQRIFood project coordinator Christian Bugge Henriksen, University of Copenhagen, and the whole project consortium including university and industry partners. Special thanks goes to Carlsberg A/S for providing co-funding and the project partners responsible for field trials (Linda Kærgaard Nielsen, Sejet Plant Breeding and Inger Bertelsen, Innovation Centre for Organic Farming) and for sample preparation (Maria Monrad Rieckmann and Lisbeth Tina Dahl, University of Copenhagen). This research was a part of the AQRIFood project, which received funding from Innovation Fund Denmark via the INNOMISSION 3 Partnership AgriFoodTure program (grant no. 1152-00001B). The authors also acknowledge financial support from the Novo Nordisk Foundation for the project "PROFERMENT: Solid-state fermentations for protein transformations and palatability of plant-based foods" (grant NNF21OC0066330). Data were generated using research infrastructure at the University of Copenhagen, including infrastructure funded from FOODHAY (Food and Health Open Innovation Laboratory, Danish Roadmap for Research Infrastructure).

Author contributions

P.T.: Conceptualization, Writing – original draft, Writing – review & editing, Visualization, Validation, Software, Investigation, Formal analysis; **S.A.K.:** Writing – review & editing, Writing – original draft, Visualization, Software, Methodology, Investigation, Formal analysis, Data curation, Conceptualization. **S.B.E:** Writing – review & editing, Conceptualization. **K.H.L.:** Writing – review &

editing, Conceptualization. **B.K.:** Writing – review & editing, Writing – original draft, Supervision, Resources, Methodology, Investigation, Conceptualization.

Competing Interests

The authors declare no competing interests.

References

(1) Pimentel, D.; Pimentel, M. Sustainability of meat-based and plant-based diets and the environment. *The American Journal of Clinical Nutrition* **2003**, *78*, 660S-663S.
(2) Willett, W.; Rockström, J.; Loken, B.; Springmann, M.; Lang, T.; Vermeulen, S.; Garnett, T.; Tilman, D.; DeClerck, F.; Wood, A.; et al. Food in the anthropocene: The eat–lancet commission on healthy diets from sustainable food systems. *The Lancet* **2019**, *393*, 447-492.
(3) Clemens, R.; van Klinken, B. J.-W. The future of oats in the food and health continuum. *British journal of nutrition* **2014**, *112*, S75-S79.
(4) Shewry, P. R.; Piironen, V.; Lampi, A.-M.; Nyström, L.; Li, L.; Rakszegi, M.; Fraś, A.; Boros, D.; Gebruers, K.; Courtin, C. M.; et al. Phytochemical and fiber components in oat varieties in the healthgrain diversity screen. *Journal of Agricultural and Food Chemistry* **2008**, *56*, 9777-9784.
(5) Khakimov, B.; Jespersen, B. M.; Engelsen, S. B. Comprehensive and comparative metabolomic profiling of wheat, barley, oat and rye using gas chromatography-mass spectrometry and advanced chemometrics. *Foods* **2014**, *3*, 569-585.
(6) Alemayehu, G. F.; Forsido, S. F.; Tola, Y. B.; Amare, E. Nutritional and phytochemical composition and associated health benefits of oat (avena sativa) grains and oat-based fermented food products. *ScientificWorldJournal* **2023**, *2023*, 2730175.
(7) Magnucka, E. G.; Kulczycki, G.; Bujak, H.; Pietr, S. J. Genotype and environment shape the free and bound phenolics and lipid content in oat (avena sativa l.) grains. *Agronomy* **2025**, *15*, 1400.
(8) EFSA. Scientific opinion on the substantiation of a health claim related to oat beta glucan and lowering blood cholesterol and reduced risk of (coronary) heart disease pursuant to article 14 of regulation (ec) no 1924/2006. *EFSA Journal* **2010**, *8*, 1885.
(9) FDA. Department of health and human services.(1997). Food labeling: Health claims. Oat and coronary heart disease: Final ruling. *Federal Register* **1997**, *62*, 3584.
(10) Martínez-Villaluenga, C.; Peñas, E. Health benefits of oat: Current evidence and molecular mechanisms. *Current Opinion in Food Science* **2017**, *14*, 26-31.
(11) Meemken, E.-M.; Qaim, M. Organic agriculture, food security, and the environment. *Annual Review of Resource Economics* **2018**, *10*, 39-63.
(12) Tal, A. Making conventional agriculture environmentally friendly: Moving beyond the glorification of organic agriculture and the demonization of conventional agriculture. *Sustainability* **2018**, *10*, 1078.
(13) Viana, L. R.; Dessureault, P.-L.; Marty, C.; Loubet, P.; Levasseur, A.; Boucher, J.-F.; Paré, M. C. Would transitioning from conventional to organic oat grains production reduce environmental impacts? A lca case study in north-east canada. *Journal of Cleaner Production* **2022**, *349*, 131344.
(14) Morcia, C.; Finocchiaro, F.; Delbono, S.; Ghizzoni, R.; Reggiani, F.; Carnevali, P.; Tumino, G.; Carrara, I.; Terzi, V. Oats: Nutritional uniqueness and breeding of a healthy superfood. In *Compendium of crop genome designing for nutraceuticals*, Kole, C. Ed.; Springer Nature Singapore, 2023; pp 153-193.
(15) Capouchova, I.; Buresova, B.; Paznocht, L.; Eliasova, M.; Pazderu, K.; Konvalina, P.; Satransky, M.; Dvoracek, V. Antioxidant activity and content of selected antioxidant compounds in grain of different oat cultivars. *Plant, Soil and Environment* **2020**, *66*, 327-333.

(16) Hao, Y.; Zhang, Z.; Luo, E.; Yang, J.; Wang, S. Plant metabolomics: Applications and challenges in the era of multi-omics big data. *aBIOTECH* **2025**, *6*, 116-132.
(17) Allwood, J. W.; Martinez-Martin, P.; Xu, Y.; Cowan, A.; Pont, S.; Griffiths, I.; Sungurtas, J.; Clarke, S.; Goodacre, R.; Marshall, A.; et al. Assessing the impact of nitrogen supplementation in oats across multiple growth locations and years with targeted phenotyping and high-resolution metabolite profiling approaches. *Food Chemistry* **2021**, *355*, 129585.
(18) Hu, H.; Campbell, M. T.; Yeats, T. H.; Zheng, X.; Runcie, D. E.; Covarrubias-Pazaran, G.; Broeckling, C.; Yao, L.; Caffe-Treml, M.; Gutiérrez, L. A.; et al. Multi-omics prediction of oat agronomic and seed nutritional traits across environments and in distantly related populations. *Theor Appl Genet* **2021**, *134*, 4043-4054.
(19) Campbell, M. T.; Hu, H.; Yeats, T. H.; Caffe-Treml, M.; Gutiérrez, L.; Smith, K. P.; Sorrells, M. E.; Gore, M. A.; Jannink, J.-L. Translating insights from the seed metabolome into improved prediction for lipid-composition traits in oat (avena sativa l.). *Genetics* **2021**, *217*.
(20) Dimberg, L. H.; Gissén, C.; Nilsson, J. Phenolic compounds in oat grains (avena sativa l.) grown in conventional and organic systems. *AMBIO: A Journal of the Human Environment* **2005**, *34*, 331-337, 337.
(21) Dvořáček, V.; Jágr, M.; Kotrbová Kozak, A.; Capouchová, I.; Konvalina, P.; Faměra, O.; Hlásná Čepková, P. Avenanthramides: Unique bioactive substances of oat grain in the context of cultivar, cropping system, weather conditions and other grain parameters. *Plants* **2021**, *10*, 2485.
(22) Pretorius, C. J.; Dubery, I. A. Avenanthramides, distinctive hydroxycinnamoyl conjugates of oat, avena sativa l.: An update on the biosynthesis, chemistry, and bioactivities. *Plants* **2023**, *12*, 1388.
(23) Sumner, L. W.; Amberg, A.; Barrett, D.; Beale, M. H.; Beger, R.; Daykin, C. A.; Fan, T. W.-M.; Fiehn, O.; Goodacre, R.; Griffin, J. L. Proposed minimum reporting standards for chemical analysis: Chemical analysis working group (cawg) metabolomics standards initiative (msi). *Metabolomics* **2007**, *3*, 211-221.
(24) Reinhard, K.; Matern, U. The biosynthesis of phytoalexins in dianthus caryophyllus l. Cell cultures: Induction of benzoyl-coa:Anthranilate n-benzoyltransferase activity. *Archives of Biochemistry and Biophysics* **1989**, *275*, 295-301.
(25) Li, Z.; Chen, Y.; Meesapyodsuk, D.; Qiu, X. The biosynthetic pathway of major avenanthramides in oat. *Metabolites* **2019**, *9*, 163.
(26) Azarbad, H. Conventional vs. Organic agriculture–which one promotes better yields and microbial resilience in rapidly changing climates? *Frontiers in Microbiology* **2022**, *Volume 13 - 2022*.
(27) Omondi, E. C.; Wagner, M.; Mukherjee, A.; Nichols, K. Long-term organic and conventional farming effects on nutrient density of oats. *Renewable Agriculture and Food Systems* **2022**, *37*, 113-127.
(28) Madajska, K.; Tratwal, A.; Roik, K.; Pietrusińska-Radzio, A.; Bocianowski, J. Evaluation of oat varieties under different levels of fertilization and crop protection in conventional and organic systems. *Agriculture* **2025**, *15*, 2538.
(29) Pichler, E. C.; Witlaczil, R.; Hofinger-Horvath, A.; Jágr, M.; Čepková, P. H.; D´Amico, S.; Grausgruber, H.; Dvořáček, V.; Schönlechner, R. Phenolic compounds, including avenanthramides, and antioxidant properties in conventionally and organically grown oat cultivars affected by germination. *Journal of Agriculture and Food Research* **2025**, *23*, 102299.
(30) Xue, Z.; Wang, B.; Qu, C.; Tao, M.; Wang, Z.; Zhang, G.; Zhao, M.; Zhao, S. Response of salt stress resistance in highland barley (hordeum vulgare l. Var. Nudum) through phenylpropane metabolic pathway. *Plos one* **2023**, *18*, e0286957.
(31) Campos, L.; Lisón, P.; López-Gresa, M. P.; Rodrigo, I.; Zacarés, L.; Conejero, V.; Bellés, J. M. Transgenic tomato plants overexpressing tyramine n-hydroxycinnamoyltransferase exhibit elevated hydroxycinnamic acid amide levels and enhanced resistance to pseudomonas syringae. *Molecular Plant-Microbe Interactions* **2014**, *27*, 1159-1169.

(32) Yu, P.; McKinnon, J. J.; Maenz, D. D.; Racz, V. J.; Christensen, D. A. The specificity and the ability of aspergillus feruloyl esterase to release p-coumaric acid from complex cell walls of oat hulls. *Journal of Chemical Technology & Biotechnology* **2004**, *79*, 729-733.
(33) Gunnaiah, R.; Kushalappa, A. C.; Duggavathi, R.; Fox, S.; Somers, D. J. Integrated metabolo-proteomic approach to decipher the mechanisms by which wheat qtl (fhb1) contributes to resistance against fusarium graminearum. *PloS one* **2012**, *7*, e40695.
(34) Yang, J.; Wang, P.; Wu, W.; Zhao, Y.; Idehen, E.; Sang, S. Steroidal saponins in oat bran. *J. Agric. Food. Chem.* **2016**, *64*, 1549-1556.
(35) Weissenberg, M.; Levy, A.; Svoboda, J. A.; Ishaaya, I. The effect of some solanum steroidal alkaloids and glycoalkaloids on larvae of the red flour beetle, tribolium castaneum, and the tobacco hornworm, manduca sexta. *Phytochemistry* **1998**, *47*, 203-209.
(36) Abbas, G.; Rauf, K.; Mahmood, W. Saponins: The phytochemical with an emerging potential for curing clinical depression. *Natural product research* **2015**, *29*, 302-307.
(37) El Aziz, M. M. A.; Ashour, A. S.; Melad, A. S. G. A review on saponins from medicinal plants: Chemistry, isolation, and determination. *J. Nanomed. Res* **2019**, *8*, 282-288.
(38) Hu, C.; Tang, Y.; Snooks, H. D.; Sang, S. Novel steroidal saponins in oat identified by molecular networking analysis and their levels in commercial oat products. *J. Agric. Food. Chem.* **2021**, *69*, 7084-7092.
(39) Bittremieux, W.; Avalon, N. E.; Thomas, S. P.; Kakhkhorov, S. A.; Aksenov, A. A.; Gomes, P. W. P.; Aceves, C. M.; Caraballo-Rodríguez, A. M.; Gauglitz, J. M.; Gerwick, W. H.; et al. Open access repository-scale propagated nearest neighbor suspect spectral library for untargeted metabolomics. *Nature Communications* **2023**, *14*, 8488.
(40) Liu, Y.; Liang, F.; Cui, L.; Xia, M.; Zhao, L.; Yang, Y.; Shi, J.; Abliz, Z. Multi-stage mass spectrometry of furostanol saponins combined with electrospray ionization in positive and negative ion modes. *Rapid Communications in Mass Spectrometry* **2004**, *18*, 235-238.
(41) Kwon, R. H.; Lee, S.; Kim, J. H.; Na, H.; Lee, S.-J.; Kim, H.-W.; Wee, C.-D.; Yoo, S. M.; Lee, S. H. Characterization of seven new steroidal saponins from korean oat cultivars by uplc-qtof-ms and uplc-ms/ms. *ACS Omega* **2024**, *9*, 14356-14367.
(42) Morrissey, J. P.; Wubben, J. P.; Osbourn, A. E. Stagonospora avenae secretes multiple enzymes that hydrolyze oat leaf saponins. *Mol Plant Microbe Interact* **2000**, *13*, 1041-1052.
(43) Miyagawa, H.; Ishihara, A.; Nishimoto, T.; Ueno, T.; Mayama, S. Induction of avenanthramides in oat leaves inoculated with crown rust fungus, puccinia coronata f. Sp. Avenae. *Bioscience, biotechnology, and biochemistry* **1995**, *59*, 2305-2306.
(44) Yang, Q.; Xuan Trinh, H.; Imai, S.; Ishihara, A.; Zhang, L.; Nakayashiki, H.; Tosa, Y.; Mayama, S. Analysis of the involvement of hydroxyanthranilate hydroxycinnamoyltransferase and caffeoyl-coa 3-o-methyltransferase in phytoalexin biosynthesis in oat. *Molecular plant-microbe interactions* **2004**, *17*, 81-89.
(45) Nkhata Malunga, L.; Ames, N.; Mitchell Fetch, J.; Netticadan, T.; Joseph Thandapilly, S. Genotypic and environmental variations in phenolic acid and avenanthramide content of canadian oat (avena sativa). *Food Chemistry* **2022**, *388*, 132904.
(46) Wise, M. L.; Doehlert, D. C.; McMullen, M. S. Association of avenanthramide concentration in oat (avena sativa l.) grain with crown rust incidence and genetic resistance. *Cereal Chemistry* **2008**, *85*, 639-641.
(47) Kim, H. U. Lipid metabolism in plants. MDPI: 2020; Vol. 9, p 871.
(48) Adigun, O. A.; Nadeem, M.; Pham, T. H.; Jewell, L. E.; Cheema, M.; Thomas, R. Recent advances in bio-chemical, molecular and physiological aspects of membrane lipid derivatives in plant pathology. *Plant, cell & environment* **2021**, *44*, 1-16.
(49) Ninkuu, V.; Aluko, O. O.; Yan, J.; Zeng, H.; Liu, G.; Zhao, J.; Li, H.; Chen, S.; Dakora, F. D. Phenylpropanoids metabolism: Recent insight into stress tolerance and plant development cues. *Frontiers in Plant Science* **2025**, *Volume 16 - 2025*.

(50) Kouřimská, L.; Sabolová, M.; Horčička, P.; Rys, S.; Božik, M. Lipid content, fatty acid profile, and nutritional value of new oat cultivars. *Journal of Cereal Science* **2018**, *84*, 44-48.
(51) Dinler, B. S.; Çetinkaya, H. An overview on azelaic acid: Biosynthesis, signalling and the action under stress conditions in plants. *Journal of Plant Stress Physiology* **2024**.
(52) Singh, P.; Arif, Y.; Miszczuk, E.; Bajguz, A.; Hayat, S. Specific roles of lipoxygenases in development and responses to stress in plants. *Plants (Basel)* **2022**, *11*.
(53) Bai, J.-h.; Liu, J.-h.; Zhang, N.; Yang, J.-h.; Sa, R.-l.; Wu, L. Effect of alkali stress on soluble sugar, antioxidant enzymes and yield of oat. *Journal of Integrative Agriculture* **2013**, *12*, 1441-1449.
(54) Mittler, R.; Zandalinas, S. I.; Fichman, Y.; Van Breusegem, F. Reactive oxygen species signalling in plant stress responses. *Nature Reviews Molecular Cell Biology* **2022**, *23*, 663-679.
(55) Seo, S. Y.; Kim, Y. J.; Kim, J.; Nam, M. H.; Park, K. Y. Phytosphingosine induces systemic acquired resistance through activation of sphingosine kinase. *Plant Direct* **2021**, *5*, e351.
(56) Michaelson, L. V.; Zäuner, S.; Markham, J. E.; Haslam, R. P.; Desikan, R.; Mugford, S.; Albrecht, S.; Warnecke, D.; Sperling, P.; Heinz, E.; et al. Functional characterization of a higher plant sphingolipid δ4-desaturase: Defining the role of sphingosine and sphingosine-1-phosphate in arabidopsis *Plant Physiology* **2008**, *149*, 487-498.
(57) Zienkiewicz, K.; Zienkiewicz, A. Degradation of lipid droplets in plants and algae—right time, many paths, one goal. *Frontiers in Plant Science* **2020**, *Volume 11 - 2020*.
(58) Popovici, G.; Weissenböck, G.; Bouillant, M.-L.; Dellamonica, G.; Chopin, J. Isolation and characterization of flavonoids from avena sativa l. *Zeitschrift für Pflanzenphysiologie* **1977**, *85*, 103-115.
(59) Knogge, W.; Weissenböck, G. Tissue-distribution of secondary phenolic biosynthesis in developing primary leaves of avena sativa l. *Planta* **1986**, *167*, 196-205.
(60) Brazier-Hicks, M.; Evans, K. M.; Gershater, M. C.; Puschmann, H.; Steel, P. G.; Edwards, R. The c-glycosylation of flavonoids in cereals. *J Biol Chem* **2009**, *284*, 17926-17934.
(61) Du, Y.; Chu, H.; Chu, I. K.; Lo, C. Cyp93g2 is a flavanone 2-hydroxylase required for c-glycosylflavone biosynthesis in rice *Plant Physiology* **2010**, *154*, 324-333.
(62) Lee, S.-S.; Baek, Y.-S.; Eun, C.-S.; Yu, M.-H.; Baek, N.-I.; Chung, D.-k.; Bang, M.-H.; Yang, S.-A. Tricin derivatives as anti-inflammatory and anti-allergic constituents from the aerial part of zizania latifolia. *Bioscience, Biotechnology, and Biochemistry* **2015**, *79*, 700-706.
(63) Lan, W.; Lu, F.; Regner, M.; Zhu, Y.; Rencoret, J.; Ralph, S. A.; Zakai, U. I.; Morreel, K.; Boerjan, W.; Ralph, J. Tricin, a flavonoid monomer in monocot lignification. *Plant Physiol* **2015**, *167*, 1284-1295.
(64) Wenzig, E.; Kunert, O.; Ferreira, D.; Schmid, M.; Schühly, W.; Bauer, R.; Hiermann, A. Flavonolignans from avena sativa. *Journal of Natural Products* **2005**, *68*, 289-292.

Figure legends

Figure 1. ANOVA-simultaneous component analysis (ASCA) performed on 228 metabolites annotated in MSI confidence levels 2 and 3 using MetaboScape spectral libraries and SIRIUS and show separation of 30 oat samples representing 10 cultivars (Caddy, Delfin, Dominik, Galant, Lion, Max, NORD 20/127, NORD 20/223, Oskar and Scotty) grown under organic (Hammel) and conventional practices (Sejet and Gamborg). Score plots (a) and (b) showing the separation of oat samples according to the farming practice (n = replicates × 30 samples, explained variance = 28.1%, p-value = 0.001) and cultivar (n = 3 locations × 3 replicates × 10 cultivars, explained variance = 17.5%, p-value = 0.001), respectively.

Panels (c) and (d) show the SC1 loadings for farming practice and cultivar, respectively. Loading values were normalized to a range from -1 to 1 and mapped to a color gradient which was used to encode SC1 loadings in the corresponding molecular networks. Each node in molecular network represents a metabolite and node color indicates the direction and magnitude of its SC1 loading.

Figure 2. Variation of metabolites from ten oat cultivars across the three growing locations (Hammel, Gamborg, Sejet). Heatmap (a) displays the 50 most abundant metabolites that varied significantly among locations according to one-way ANOVA with FDR-corrected $p < 0.05$. The color intensity represents the normalized relative mean abundance of each metabolite across all cultivars per location. Normalized values range from 0 to 1, where 0 (yellow) indicates lower metabolite levels, and 1 (blue) represents the highest relative mean abundance. Hierarchical clustering of metabolites is visualized as a dendrogram, which is shown on the left. (b) Variation of 12 selected metabolites with distinct relative abundance across locations. Box plots show the relative abundance of the metabolites, FDR corrected p-values and effect size (%), which are calculated from one-way ANOVA performed on the relative abundance.

Figure 3. Variation of metabolites in the ten oat cultivars independent of location. Heatmap (a) displays the 45 metabolites that varied significantly among cultivars based on one-way ANOVA with FDR-corrected $p < 0.05$. The color intensity represents the normalized relative mean abundance of each metabolite across all cultivars. Normalized values range from 0 to 1, where 0 (yellow) indicates lower metabolite levels, and 1 (blue) represents the highest relative mean abundance. Hierarchical clustering of metabolites is visualized as a dendrogram, which is shown on the left. (b) Variation of 7 selected metabolites with distinct relative abundance across cultivars. Box plots show the relative abundance of the metabolites, FDR corrected p-values and effect size (%), which are calculated from one-way ANOVA performed on the relative abundance.

Figure 4. Molecular networking and MS/MS spectra of hydroxycinnamic acid amides detected in oat grains. (a) Molecular network of hydroxycinnamic acid amides. Pie charts within nodes show the relative chromatographic peak area abundance of each compound across the three growing locations. Edges connecting nodes are labelled with the precursor ion m/z differences between the corresponding compounds. Avenanthramides are named according to the Dimberg system; f-ser denotes N-feruloylserotonin and c-ser – N-caffeoylserotonin. (b) MS/MS spectra of selected hydroxycinnamic amides showing the characteristic fragmentation pattern arising from cleavage of the amide bond linking the hydroxycinnamic acid moiety to anthranilic acids or serotonin.

Figure 5. Molecular networking and MS/MS spectra of steroidal saponins detected in oat grains. (a) Molecular network of nuatigenin-type (furospirost-5-en-3β,26-diol) steroidal saponins referred to as avenacosides and furostane-type (furost-5-en-3β,22,26-triol) steroidal saponins referred to as sativacosides. Pie charts within nodes show the relative chromatographic peak area abundance of each compound across the three growing locations. Edges connecting nodes are labelled with the precursor ion m/z differences between the corresponding compounds. (b) MS/MS spectra of the detected steroidal saponins. The spectrum of nuatigenin-3-O-Glc is omitted. Bold m/z values indicate the precursor ion.

Figure 1

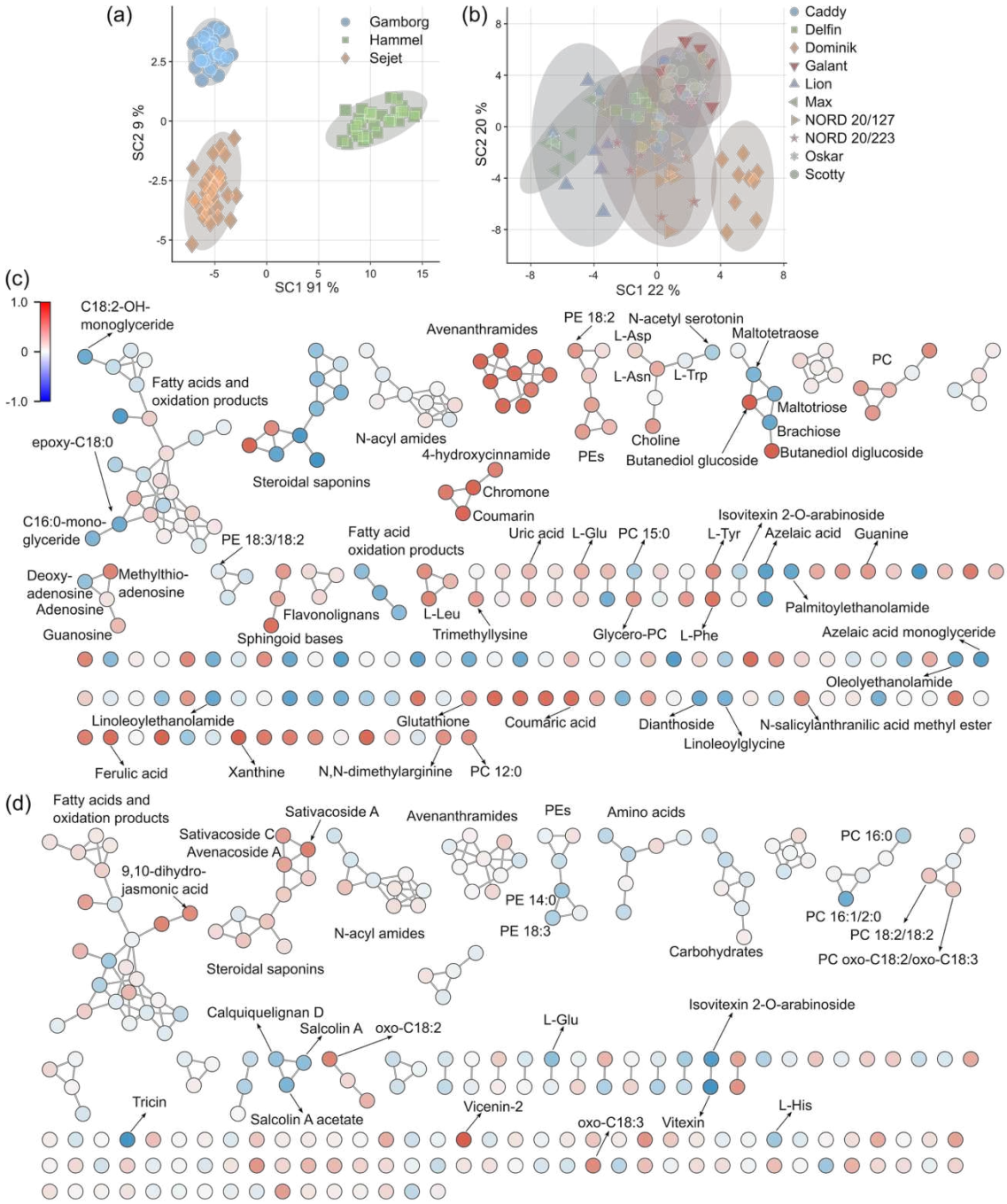

(a)
Gamborg
Hammel
Sejet
SC2 9 %
SC1 91 %
(b)
Caddy
Delfin
Dominik
Galant
Lion
Max
NORD 20/127
NORD 20/223
Oskar
Scotty
SC2 20 %
SC1 22 %
(c)
C18:2-OH-monoglyceride
Fatty acids and oxidation products
epoxy-C18:0
C16:0-mono-glyceride
PE 18:3/18:2
Deoxy-adenosine
Methylthio-adenosine
Adenosine
Guanosine
Steroidal saponins
Avenanthramides
N-acyl amides
4-hydroxycinnamide
Chromone
Coumarin
Flavonolignans
Sphingoid bases
Fatty acid oxidation products
L-Leu
Trimethyllysine
PE 18:2
N-acetyl serotonin
L-Asp
L-Asn
L-Trp
PEs
Choline
Maltotetraose
Maltotriose
Brachiose
Butanediol glucoside
Butanediol diglucoside
PC
Uric acid
L-Glu
PC 15:0
Glycero-PC
L-Tyr
L-Phe
Isovitexin 2-O-arabinoside
Azelaic acid
Guanine
Palmitoylethanolamide
Azelaic acid monoglyceride
Oleoylethanolamide
N-salicylanthranilic acid methyl ester
Linoleoylglycine
Linoleoylethanolamide
Ferulic acid
Xanthine
Glutathione
N,N-dimethylarginine
Coumaric acid
Dianthoside
PC 12:0
(d)
Fatty acids and oxidation products
9,10-dihydro-jasmonic acid
Sativacoside A
Sativacoside C
Avenacoside A
Steroidal saponins
N-acyl amides
Avenanthramides
PEs
PE 14:0
PE 18:3
Amino acids
Carbohydrates
PC 16:0
PC 16:1/2:0
PC 18:2/18:2
PC oxo-C18:2/oxo-C18:3
Calquiquelignan D
Salcolin A
oxo-C18:2
Salcolin A acetate
Tricin
L-Glu
Isovitexin 2-O-arabinoside
Vicenin-2
oxo-C18:3
Vitexin
L-His

Figure 2

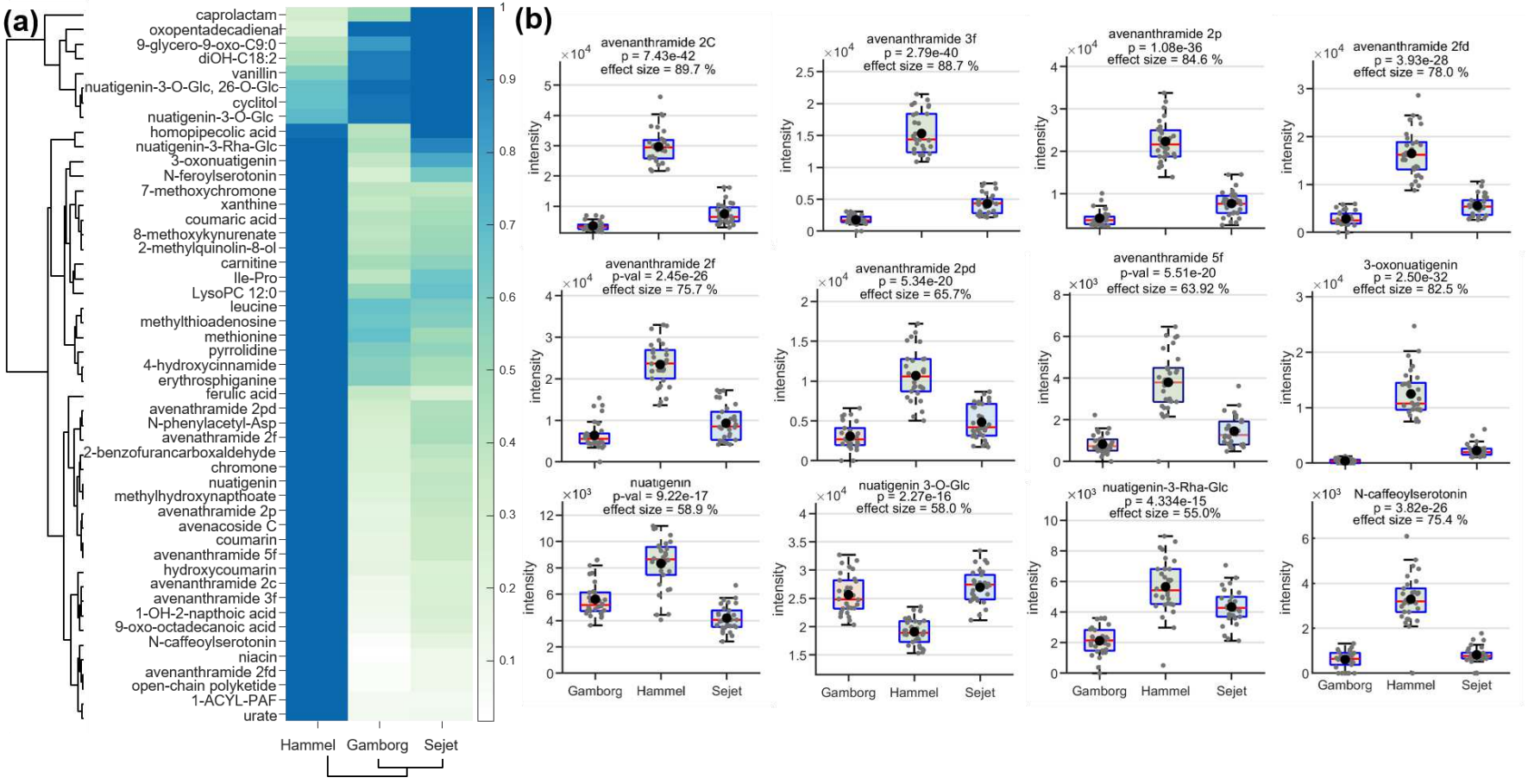

(a)
caprolactam
oxopentadecadienal
9-glycero-9-oxo-C9:0
diOH-C18:2
vanillin
nuatigenin-3-O-Glc, 26-O-Glc
cyclitol
nuatigenin-3-O-Glc
homopipecolic acid
nuatigenin-3-Rha-Glc
3-oxonuatigenin
N-feroylserotonin
7-methoxychromone
xanthine
coumaric acid
8-methoxykynurenate
2-methylquinolin-8-ol
carnitine
Ile-Pro
LysoPC 12:0
leucine
methylthioadenosine
methionine
pyrrolidine
4-hydroxycinnamide
erythrosphiganine
ferulic acid
avenathramide 2pd
N-phenylacetyl-Asp
avenathramide 2f
2-benzofurancarboxaldehyde
chromone
nuatigenin
methylhydroxynapthoate
avenathramide 2p
avenacoside C
coumarin
avenanthramide 5f
hydroxycoumarin
avenanthramide 2c
avenanthramide 3f
1-OH-2-napthoic acid
9-oxo-octadecanoic acid
N-caffeoylserotonin
niacin
avenanthramide 2fd
open-chain polyketide
1-ACYL-PAF
urate
1
0.9
0.8
0.7
0.6
0.5
0.4
0.3
0.2
0.1
Hammel
Gamborg
Sejet
(b)
avenanthramide 2C
p = 7.43e-42
effect size = 89.7 %
avenanthramide 3f
p = 2.79e-40
effect size = 88.7 %
avenanthramide 2p
p = 1.08e-36
effect size = 84.6 %
avenanthramide 2fd
p = 3.93e-28
effect size = 78.0 %
avenanthramide 2f
p-val = 2.45e-26
effect size = 75.7 %
avenanthramide 2pd
p = 5.34e-20
effect size = 65.7%
avenanthramide 5f
p-val = 5.51e-20
effect size = 63.92 %
3-oxonuatigenin
p = 2.50e-32
effect size = 82.5 %
nuatigenin
p-val = 9.22e-17
effect size = 58.9 %
nuatigenin 3-O-Glc
p = 2.27e-16
effect size = 58.0 %
nuatigenin-3-Rha-Glc
p = 4.334e-15
effect size = 55.0%
N-caffeoylserotonin
p = 3.82e-26
effect size = 75.4 %
intensity
Gamborg
Hammel
Sejet

Figure 3

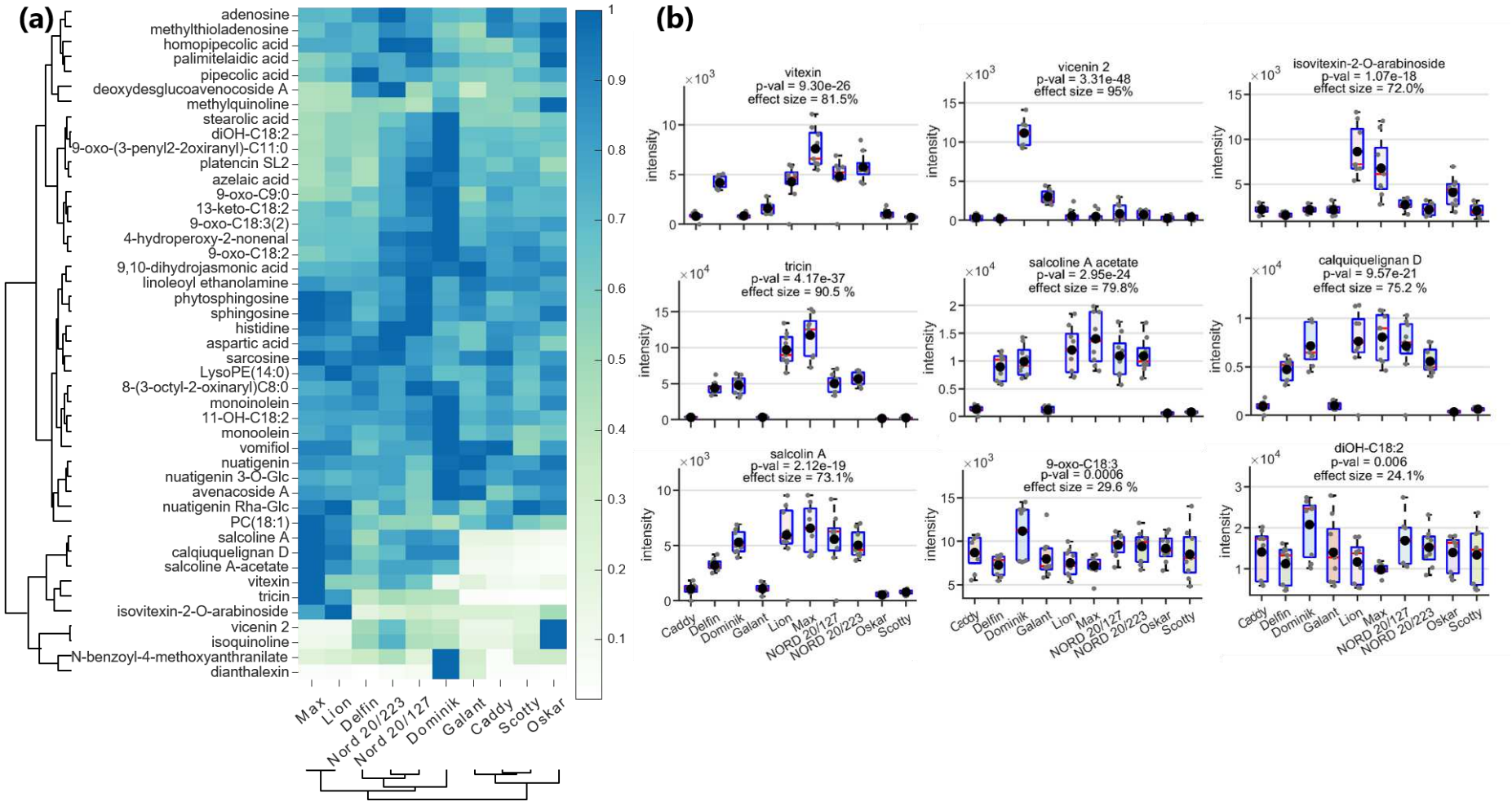

(a)
adenosine
methylthioladenosine
homopipecolic acid
palimitelaidic acid
pipecolic acid
deoxydesglucoavenocoside A
methylquinoline
stearolic acid
diOH-C18:2
9-oxo-(3-penyl2-2oxiranyl)-C11:0
platencin SL2
azelaic acid
9-oxo-C9:0
13-keto-C18:2
9-oxo-C18:3(2)
4-hydroperoxy-2-nonenal
9-oxo-C18:2
9,10-dihydrojasmonic acid
linoleoyl ethanolamine
phytosphingosine
sphingosine
histidine
aspartic acid
sarcosine
LysoPE(14:0)
8-(3-octyl-2-oxinaryl)C8:0
monoinolein
11-OH-C18:2
monoolein
vomifiol
nuatigenin
nuatigenin 3-O-Glc
avenacoside A
nuatigenin Rha-Glc
PC(18:1)
salcoline A
calqiuquelignan D
salcoline A-acetate
vitexin
tricin
isovitexin-2-O-arabinoside
vicenin 2
isoquinoline
N-benzoyl-4-methoxyanthranilate
dianthalexin
Max
Lion
Delfin
Nord 20/223
Nord 20/127
Dominik
Galant
Caddy
Scotty
Oskar
1
0.9
0.8
0.7
0.6
0.5
0.4
0.3
0.2
0.1
(b)
vitexin
p-val = 9.30e-26
effect size = 81.5%
vicenin 2
p-val = 3.31e-48
effect size = 95%
isovitexin-2-O-arabinoside
p-val = 1.07e-18
effect size = 72.0%
tricin
p-val = 4.17e-37
effect size = 90.5 %
salcoline A acetate
p-val = 2.95e-24
effect size = 79.8%
calquiquelignan D
p-val = 9.57e-21
effect size = 75.2 %
salcolin A
p-val = 2.12e-19
effect size = 73.1%
9-oxo-C18:3
p-val = 0.0006
effect size = 29.6 %
diOH-C18:2
p-val = 0.006
effect size = 24.1%
intensity
Caddy
Delfin
Dominik
Galant
Lion
Max
NORD 20/127
NORD 20/223
Oskar
Scotty

Figure 4

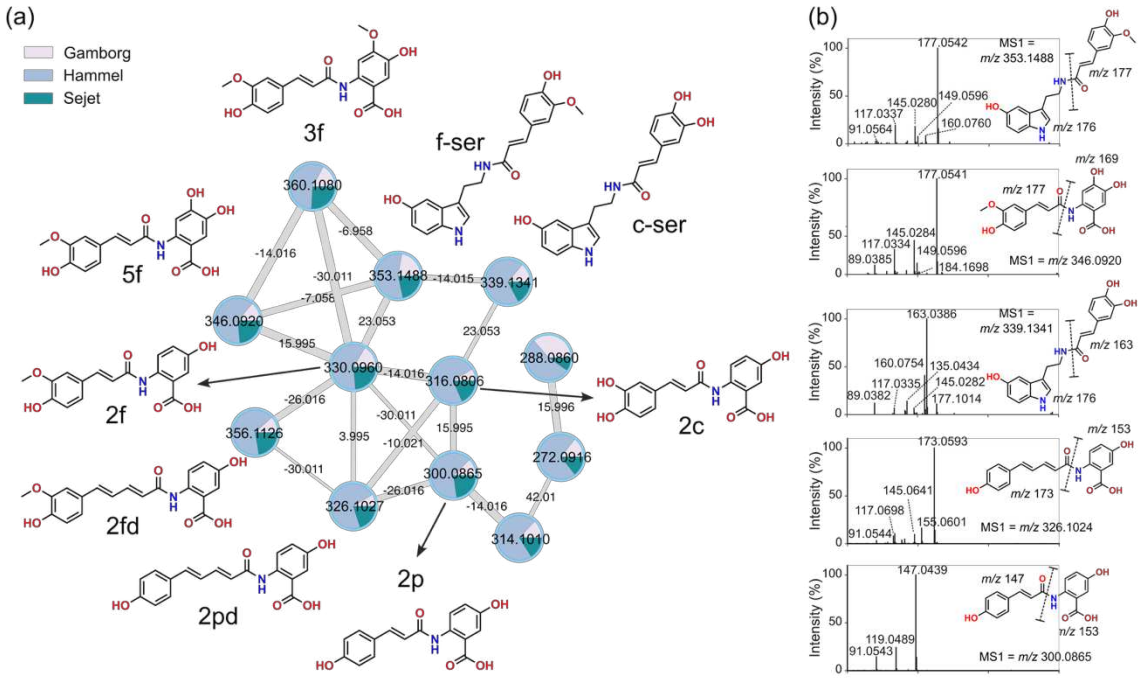
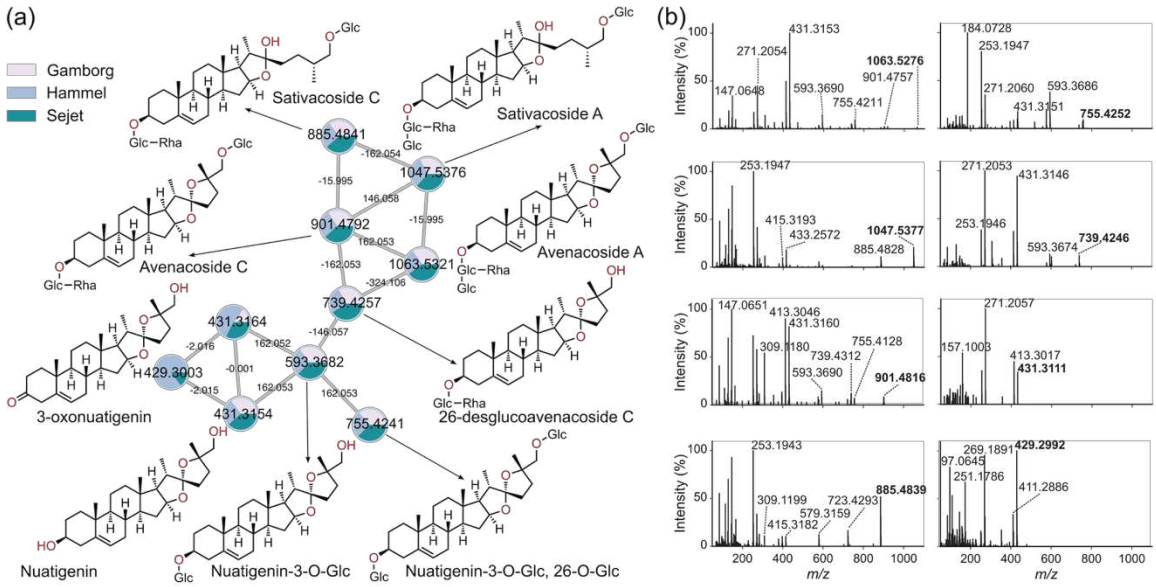
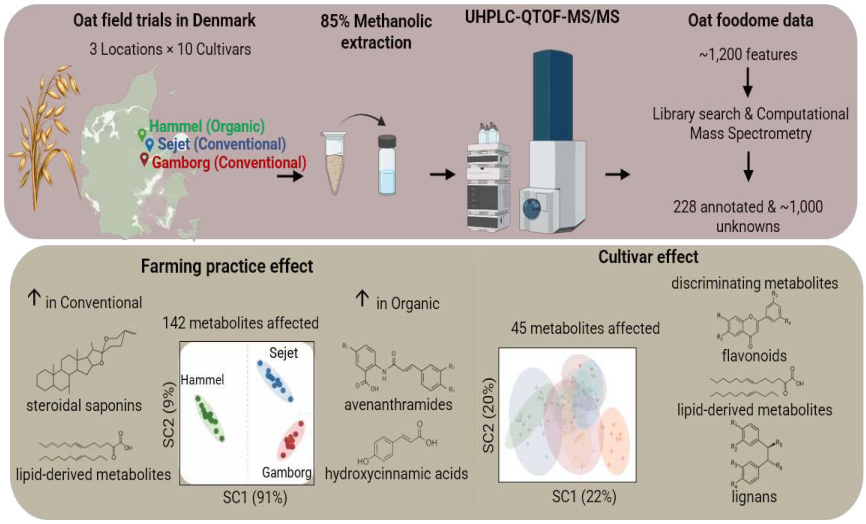

(a)
Gamborg
Hammel
Sejet
3f
f-ser
c-ser
5f
2f
2fd
2pd
2p
2c
360.1080
353.1488
339.1341
346.0920
330.0960
316.0806
288.0860
356.1126
326.1027
300.0865
272.0916
314.1010
-6.958
-14.016
-30.011
-14.015
-7.056
23.053
15.995
-26.016
-10.021
3.995
42.01
15.996
(b)
MS1 = m/z 353.1488
MS1 = m/z 346.0920
MS1 = m/z 339.1341
MS1 = m/z 326.1024
MS1 = m/z 300.0865
Intensity (%)

Figure 5


(a)
Gamborg
Hammel
Sejet
Sativacoside C
Sativacoside A
Avenacoside C
Avenacoside A
26-desglucoavenacoside C
3-oxonuatigenin
Nuatigenin
Nuatigenin-3-O-Glc
Nuatigenin-3-O-Glc, 26-O-Glc
885.4841
1047.5376
901.4792
1063.5321
739.4257
431.3164
429.3003
431.3154
593.3682
755.4241
(b)
Intensity (%)
m/z

Graphical abstract



Supplementary Files

This is a list of supplementary files associated with this preprint. Click to download.

- SupportingInformation.pdf